

On the interaction between corrosion and fatigue which determines the remaining life of bridges

[D. Peng](#)

[R. Jones](#)

[R.R.K. Singh](#)

[F. Berto](#)

[A.J. McMillan](#)

Abstract

This paper studies the prior effect of corrosion on fatigue on the growth of cracks that arise from natural corrosion in steel bridges. It is shown that these 2 effects need to be simultaneously analysed. If not, then the resulting life is not conservative. This paper presents a simple methodology for performing this coupled analysis.

1 INTRODUCTION

It has long been known that the corrosion of steel bridges can have a marked effect on structural integrity. Indeed, following the collapse of the I35W bridge in Minneapolis and the introduction by US Rep. Michael Conway (R-TX11) of the Bridge Life Extension Act of 2008 Transportation for America subsequently conducted an analysis of the US National Bridge Inventory¹ and reported that 1 in 9 US bridges were structurally deficient. In this context, it should be noted that for steel bridges, the primary problems essentially result from either corrosion due to exposure of the steel to atmospheric conditions and/or from the growth of cracks that arise as a result of small nondetectable initial material discontinuities.² As a result, the US National Cooperative Highway Research Program, NCHRP Synthesis study,² highlighted the need to develop advanced fatigue life calculation procedures that were capable of accounting for nonvisible cracks in steel bridges. The need to be able to account for small submillimetre initial defects is reinforced in the US Federal Highway Administration Steel Bridge Design Handbook³ where it was noted that crack growth essentially starts from day one and that the majority of the life of steel bridges is consumed in growing to a size where a crack can be detected. As explained in,⁴ this observation coincides with that seen in the growth of cracks in operational aircraft.^{5, 6}

In this context, it is now known that the da/dN versus ΔK relationship associated with the growth of cracks in bridge steels and in the high strength aerospace steels D6ac and 4340 steel are similar and can be represented by the same Nasgro equation.[4](#), [7](#) Furthermore, it is also known that crack growth in bridge steels repaired with an externally bonded composite patch falls on the same “master curve” as does crack growth in operational aircraft and also the growth of cracks in aluminium alloys repaired with an externally bonded composite patch.[7](#)

The need to accurately compute the growth of small submillimetre cracks in bridge steels was addressed in[4](#) which revealed that the crack growth history associated with cracks that arose and grew from natural corrosion in a section of a badly corroded steel bridge could be predicted as per[8](#) by using the Hartman-Schive variant of the Nasgro equation, viz:

$$da/dN = D ((\Delta K - \Delta K_{thr}) / \sqrt{(1 - K_{max}/A)})^p \quad (1)$$

As shown in[4](#) for bridge steels we have $D = 1.5 \times 10^{-10}$ and $p = 2$. Furthermore for cracks that arise and grow from small naturally occurring material discontinuities, we need to set the threshold term ΔK_{thr} to a small value, see[4](#), [8](#) for more details. Here, A is the cyclic fracture toughness and ΔK and K_{max} are the range of the stress intensity and the maximum value of the stress intensity factor in a cycle, respectively, see[4](#), [8](#) for more details.

Turning to the question of surface corrosion on crack growth in steel bridges, it should be noted that a detailed discussion of the field of corrosion fatigue in steel is provided in[9](#). However, there are only a few available publications on the problems of existing surface corrosion on crack growth in steel bridges. A probabilistic approach which used a damage stress model to predict fatigue lives was developed in[10](#). Other methods are focused on the use of S-N curves, which use corrosion rates and cumulative fatigue damage approaches,[11](#), [12](#) for different atmospheric conditions. A fatigue crack growth evaluation method based on linear elastic fracture mechanics was developed in[13](#). No available solutions can be found in the literature for the simultaneous effect of material loss due to corrosion and fatigue crack growth due to traffic loads.

The prediction of the fatigue life of a corroded bridge steel beam is both difficult and computationally intensive as calculations need to be made at each stage of the life of the beam. This is due to the need to compute the stress intensity factors for each crack

configuration, to calculate the amount of crack growth, update the crack geometry, and then re-compute the stress intensity factors for this new geometry. This problem, in the absence of corrosion, was discussed in detail in [8](#) which presented the fundamental steps needed to compute the crack growth histories associated with naturally occurring cracks in complex geometries subjected to representative operational load spectra. The steps associated with the analysis outlined in [8](#) can be summarised as:

- a. Perform a finite element analysis of the uncracked structure.
- b. Extract the stresses at the fatigue critical locations
- c. Use 3D, or 2D weight functions, [14-17](#) or alternatively Trefftz function solutions [18-20](#) to compute the $K(a, c)$ solution space. Here, “a” is the crack depth and “c” is the surface crack length. This generally takes less than 5 minutes on a laptop or a PC. Examples of this technique as applied to cracking in sideframes, couplers, and rail wheels are given in [14](#), [17](#) and examples associated with cracking in aerospace materials are given in [8](#), [21](#)
- d. Use the Hartman-Schijve variant of the NASGRO together with the $K(a, c)$ solution space determined above and the associated load spectrum to compute the crack length/depth versus cycles history.

However, as explained in [8](#) when analysing the more complex problem of the simultaneous occurrence of corrosion and cracks in aging rail bridges, the above process needs to be modified to also allow for the reduction in the section thickness as the bridge corrodes. This (unfortunately) means that a range of uncracked models, with different section thicknesses, need to be created and the solution space $K(a, c)$ determined for each. The crack growth analysis then uses the measured (worse case) steady-state corrosion rate for the bridge to determine the amount of material that has been lost and interpolates between the various $K(a, c)$ solution spaces to determine the appropriate stress intensity factors to use to grow the crack.

To illustrate this process, the present paper discusses issues associated with fatigue crack growth in a corroded steel beam. As per the approach outlined in steps a) to d), the first step in the analysis is to create a 3D model of the steel bridge beam without corrosion and to analyse the region of interest. In this initial model, the crack is not explicitly modelled.

Steps b) to c) are then used to determine the stress intensity factors (K) for any given crack geometry. These stress intensity factors are then used in conjunction with equation (1) to compute the crack growth history, ie, step d). In this analysis, as outlined in [8](#) for each increment in crack growth, the rate of loss of material due to corrosion is

simultaneously computed and the crack geometry, ie, after allowing for the associated loss of material, is determined/adjusted as is the new stress state in the reduced section thickness. This process is then continued until failure by either fracture or by exceeding the ultimate strength of the remaining ligament occurs.

An advantage of this approach is that it negates the need to explicitly model cracks, see [8](#), [14](#), [17](#). A crack of any size can be analysed using the original (un-cracked) finite element model. As cracks are not modelled explicitly, a coarser mesh can be used to minimise the number of degrees of freedom, thereby reducing the analysis time. Solutions for the stress-intensity factors can then be obtained for a variety of cracks using the original finite element analysis.

To illustrate how this approach can be used to compute the growth of cracks that arise due to natural corrosion in bridge steels, a simplified analysis of a section of V/Line Bridge 62 in Kilmore East, Victoria, Australia is performed. By comparing the life obtained by (1) allowing only for corrosion and (2) by performing a coupled corrosion-fatigue analysis, we find that method (1) is unconservative. We also show that the interaction between fatigue crack growth and the stress increase created by corrosion-induced section reduction needs to be considered when assessing the remaining life of an aged steel bridge.

2 THE AASHTO CORROSION STANDARD

Before we can assess the coupled effect of corrosion and fatigue, we first need a knowledge of the rate of corrosion. In this paper, we will adopt the American Association of State Highway and Transportation Officials (AASHTO) recommended metal loss model [22](#), [23](#) which states that the metal loss versus time curve is bilinear, see Figure [1](#). However, the data shown in Figure [1](#) are not particularly convincing. Nevertheless, this approach to assessing the “steady-state” corrosion rate is consistent with the International Standard *Corrosion of Metals and Alloys—Corrosivity of Atmospheres*, ISO designation 9224, [24](#) which specifies guiding values of corrosion rate for metals exposed to the atmosphere consisting of an average corrosion rate during the first 10 years of exposure. A detailed review of the corrosion of bridge steels, the AASHTO and ISO corrosion standards, and documented steady state corrosion rates associated with a range of locations and steels is in given in [25](#).

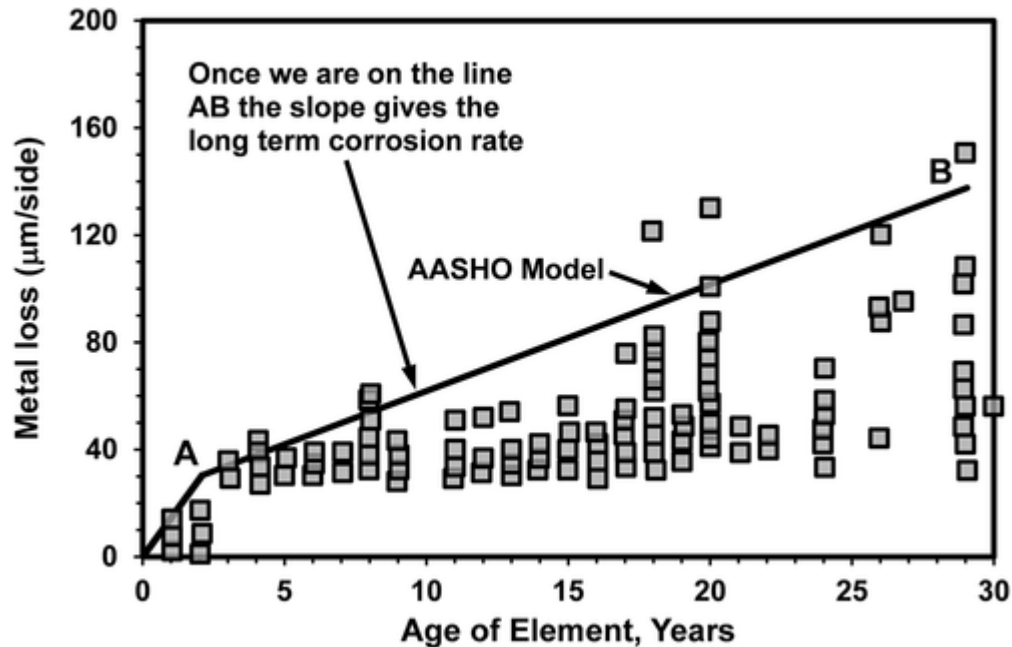


Figure 1

[Open in figure viewerPowerPoint](#)

An example of the bilinear metal loss versus time curve, from [22](#)

One problem with aging bridges is that if there is any serious corrosion, it is likely to have developed over a reasonable number of years. However, to know its significance, we need to know how fast the bridge is corroding, ie, its corrosion rate, at this moment in time. That said you do not have the luxury to locate corrosion sensors or weight loss samples on a bridge and wait for a further 5 years or so until the sensors/samples themselves reach the steady-state corrosion rate that the bridge is seeing. You need answers much sooner.

The advantage of the AASHTO bilinear approach is that once the bridge is behaving such that the metal loss versus time curve is on the line AB in Figure 1 you know the long-term corrosion rate without having to monitor the bridge for years. For bridges, this can be done in the order of 4 to 12 months using electrical resistance corrosion sensors. [26](#) To this end, a steel electrical resistance corrosion sensor was used to measure the metal loss in Bridge 62 at Kilmore East which is inland in Victoria, Australia. The resultant metal loss versus time curve is shown in Figure 2. The steady-state corrosion rate determined in this study was 0.024 (mm/year). This rate is consistent with those documented in [25](#)

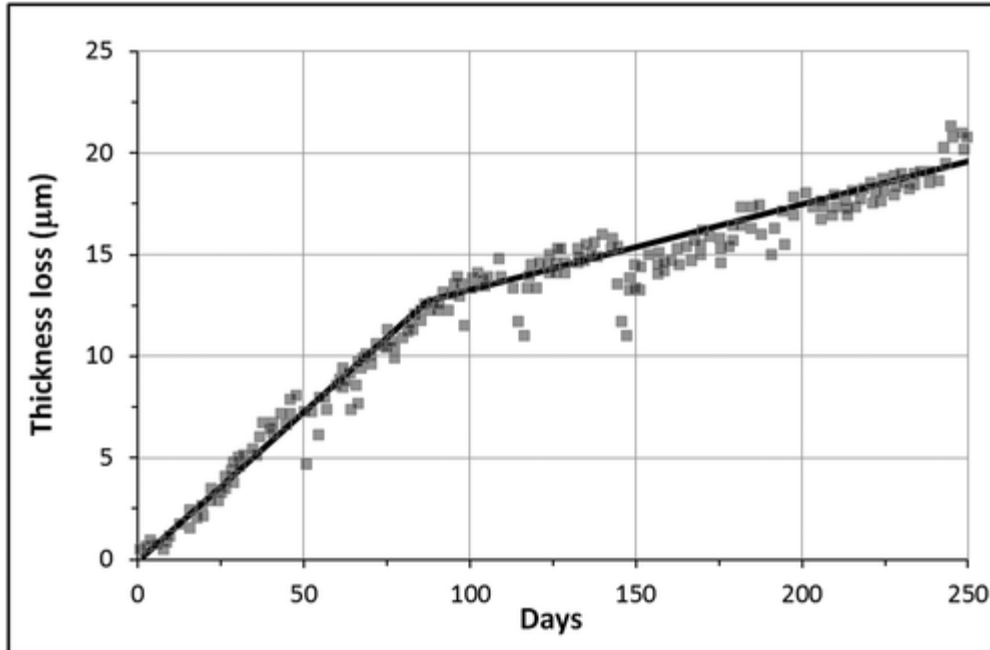


Figure 2
[Open in figure viewerPowerPoint](#)
 Measured thickness loss at East Kilmore in Victoria

The results shown in Figure 2 support the AASHTO standard for the loss of metal seen by steel bridges. As such, the AASHTO bilinear relationship between metal loss and the time in service provides a simple method for estimating the corrosion rates associated with aging structures.

3 TRAFFIC LOAD SPECTRA

As part of the corrosion measurement program mentioned previously, the strain (load) spectrum was also measured. Bridge 62 in East Kilmore saw passenger trains, including trains pulled by N Class locomotives, Sprinter carriages, and ore trains. Armed with this information and details of the number of trains per week, see Table 1, the load spectrum associated with the bridge can be determined. To this end, the associated Road Environment Percentage Occurrence Spectrum (REPOS) array used in this paper is shown in Figure 3 in the form of a 3D distribution of the percentage of occurrences.

Table 1. Data on trains using UP line over Bridge 62

Train type	Loco weight	Wagon weight	No of wagons	No per week	Total Wt/week
N class passenger	118	60	5	14	5852
Sprinter		60	2	14	1680
Ore train	128	100	20	7	14 896

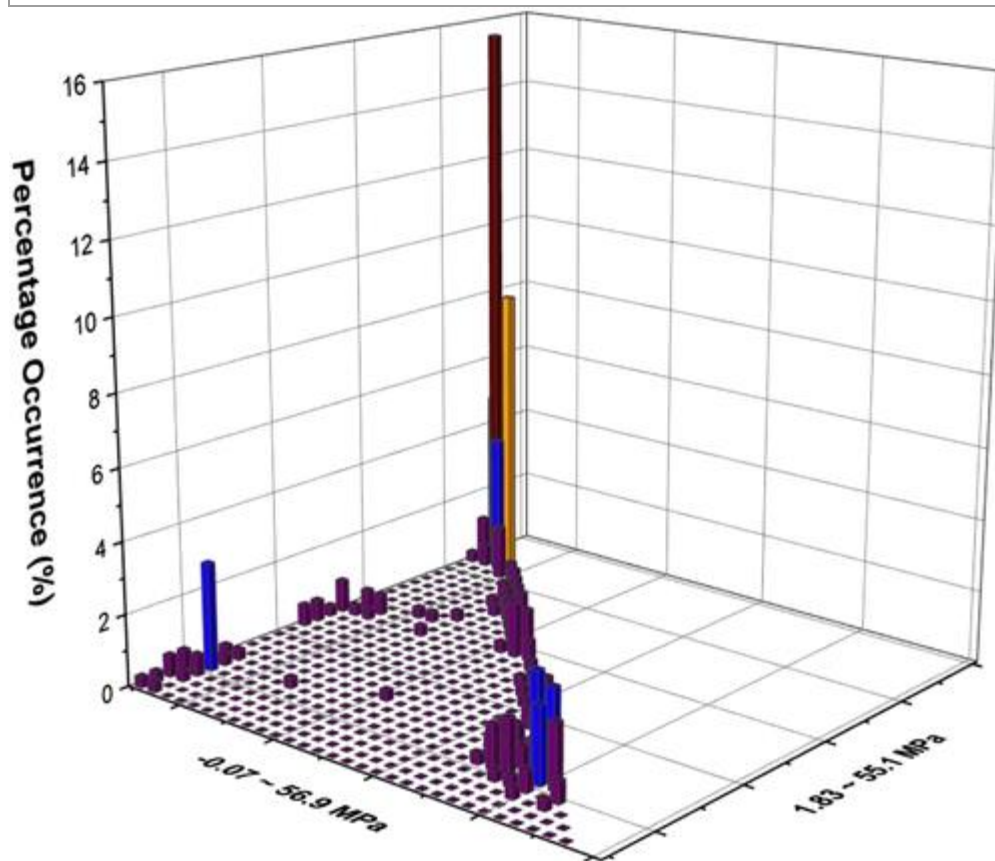


Figure 3
[Open in figure viewerPowerPoint](#)

3D bar chart of the percentage occurrence distribution measured in Bridge 62 near Kilmore East [Colour figure can be viewed at wileyonlinelibrary.com]

4 FATIGUE CRACK GROWTH WITH CORROSION EFFECT MODEL

Armed with a knowledge of the da/dN versus ΔK behaviour of bridge steels, the load spectrum, and the steady-state corrosion rate, we are now in a position to assess the combined effect of corrosion and fatigue on the remaining life of a bridge.

4.1 Failure due to material loss (corrosion)

A bending couple M applied to the section of interest creates normal stresses in the cross section, while the shear force V creates shearing stresses in that section. Corrosion of steel bridge girders will be a maximum where electrolyte can “wick” between the transom and the girder flange or where electrolyte is trapped by some other means. In general, the worst case scenario involves a loss of material from the web and/or the top and the bottom flanges. A graphical representation of the corroded I beam is provided in Figure 4. Using the equation for outer flange fibre stress in beams subject to bending:

$$\sigma_Q = My/I(2)$$

where σ is the stress, M is the applied Moment, y the distance from the beam neutral axis to the extreme flange fibre, and I is the Moment of Inertia about the neutral axis, a spread sheet can be raised to tabulate the reducing flange thickness due to corrosion and the consequential increase in the flange stresses. The limits in this assessment process are the as-new girder measured stress and the material yield stress or the buckling strength.

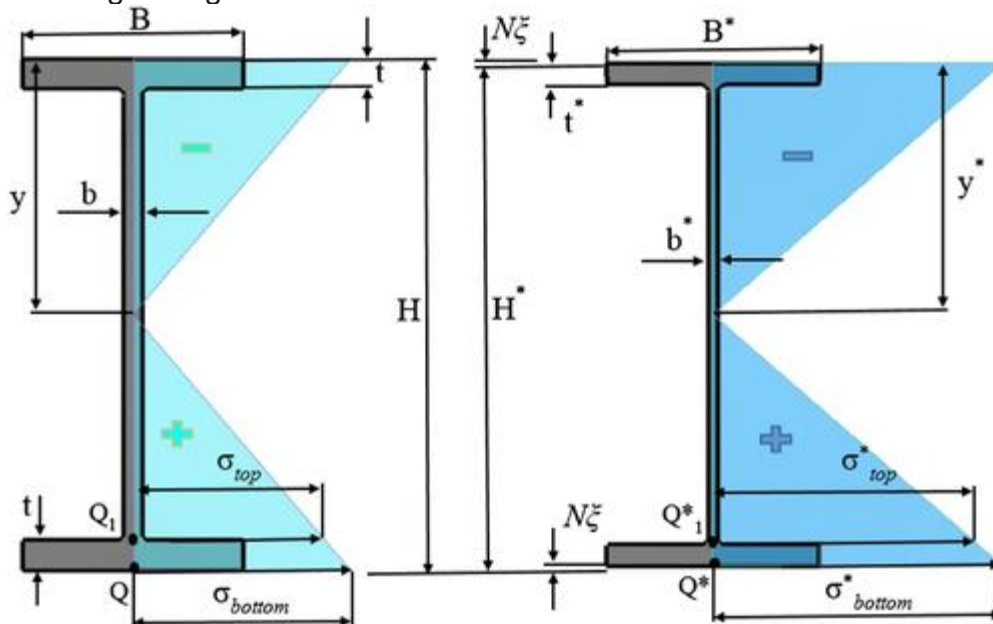


Figure 4
[Open in figure viewerPowerPoint](#)

Graphical representation of the corroded I beam [Colour figure can be viewed at wileyonlinelibrary.com]

Let us define the normal and shear stress at point Q_1 as shown in Figure 4 as σ_{Q_1} and τ_{Q_1} .

$$\sigma_{Q_1} = M(y-t)/I \quad (3)$$

$$\tau_{Q_1} = (H-t)BtV/(2bI) \quad (4)$$

With this notation the maximum principal stress at point Q_1 is:

$$\sigma_1(Q_1) = \frac{\sigma_{Q_1}}{2} + \sqrt{\left(\frac{\sigma_{Q_1}}{2}\right)^2 + (\tau_{Q_1})^2} \quad (5)$$

Therefore, the maximum stress in the flange is given by

$$\sigma = \text{Max}[\sigma_Q, \sigma_1(Q_1)] \quad (6)$$

If the measured corrosion rate for a bridge steel I beam is ξ (mm/year), the maximum stress in the I beam σ is a function of the corrosion rate ξ .

4.2 Failure due to the combined action of corrosion and fatigue on tension dominated surfaces

Because, on tension dominated surfaces, the life of the corroded steel bridge is a strong function of both the corrosion rate and the assumed initiating (inherent) crack size, this paper addresses an approximate method for estimating the effect of interaction of combined corrosion and crack growth on remaining life. In this analysis, the stress intensity factors were computed as outlined in steps b) and c) in Section 1. To this end for each iteration, as the section size reduces, the stress intensity factor for a crack in a corroded steel beam K_I is expressed in the form

$$K_I = F_\sigma K_{I(Original)}(a^*, c^*) \quad (7)$$

where, F_σ is a “geometry evolution factor”, which accounts for the reduction in the section thickness due to corrosion, and the stress intensity factor $K_{I(Original)}(a^*, c^*)$ is the value obtained using the original geometry (ie, where there is no material loss due to corrosion) and is obtained as per. 15, 16 Here (a, c) and (a*, c*) denote the crack depths and surface crack lengths without an allowance for the loss of material due to corrosion and allowing for a reduction in the section thickness due to corrosion, respectively. The crack depth “a” is related to a*, see Figure 5, by the relationship.

$$a^* = a - \xi t \quad (8)$$

where t is the current time and ξ is the corrosion rate. If we assume that the crack is a semi-elliptical surface crack, the relationship for the surface length can be approximated as

$$c^* = c\sqrt{1-(\xi t/a)^2} \quad (9)$$

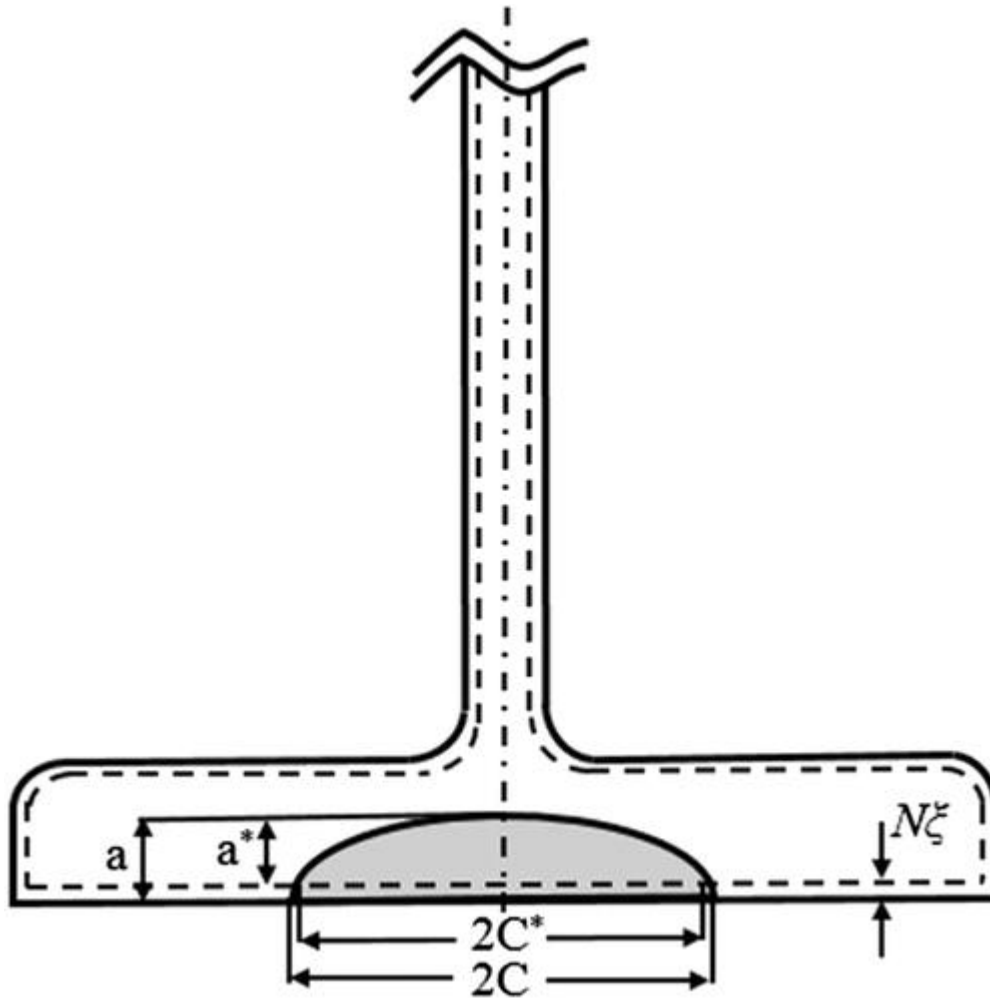


Figure 5

[Open in figure viewer](#) PowerPoint

Schematic showing a semi-elliptical crack in corroded I beam

If we assume that the rate of corrosion is the same on both the upper and lower surfaces of the beam, then the geometry evolution factor F_σ can be approximated as:

$$F_\sigma = \frac{\sigma_{bottom}^* + \sigma_{top}^*}{\sigma_{bottom} + \sigma_{top}} = \frac{2y^* - t^*}{2y - t} \frac{I}{I^*} \quad (10)$$

where I and I^* are the moment of inertia about the neutral axis with original (no corrosion) and the current corroded section, respectively.

Having determined the current section thickness and the associated stress intensity factors, equation (1), ie, the da/dN versus ΔK relationship for bridge steels, is then used to compute the new crack shape. To allow for the simultaneous loss of material due to corrosion, both the section thickness and the new crack shape are then modified to

account for the loss of material due to corrosion. The process is continued until failure either by exceeding the allowable fracture toughness of the material or by exceeding the ultimate strength of the remaining ligament. If the increment in the crack length is less than the loss of material due to corrosion, it is assumed that the crack has been “eaten” by the corrosion. In this case, the analysis continues using the assumed initial (inherent) crack size input by the user. In this fashion, the remaining life of the section can be determined.

5 NUMERICAL EXAMPLES AND RESULTS ANALYSIS

An analysis of cracking in Bridge 62 with an assumed corrosion rate of 0.024 mm/year was chosen to illustrate this approach. In this (indicative) analysis, the initiating (inherent) crack was taken from the test described in [4](#) which tested a section from a condemned and badly corroded steel bridge, to be a small 0.05-mm-deep semicircular initial crack. This size crack, which was not reported in [4](#) because the crack did not grow appreciably, was the smallest crack size found in these tests.

The substructure of Bridge 62 was subjected to significant moisture and resulting corrosion during the wet seasons, see Figure [6](#). The bridge has 2 rail tracks, each of which is supported by 4 girders with 4.87 m length. The dimensions of the girders are given in Table [2](#).



Figure 6

[Open in figure viewerPowerPoint](#)

Surface corrosion of main girders of Bridge 62 [Colour figure can be viewed at wileyonlinelibrary.com]

Table 2. Dimensions of the Bridge 62 girders

Depth	381 mm
Web thickness	12 mm
Flange width	152 mm
Flange thickness	22 mm (average)

The relationship between the maximum stress, allowing for the loss of material due to corrosion, and operational life is given in Figure 7. The yield stress for this steel was conveyed by V/Line staff to be approximately 240 MPa. This implies that retirement resulting from corrosion from an as-new state is approximately 244 years, see Figure 7.

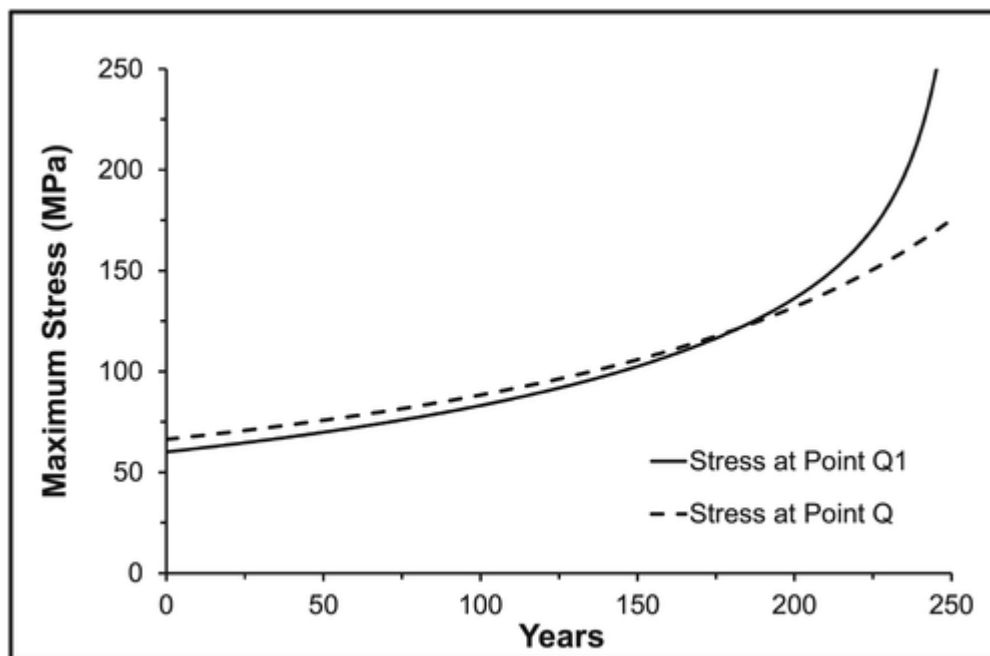


Figure 7

[Open in figure viewerPowerPoint](#)

Increase in maximum stress with time

The increase in the maximum deflection with time is shown in Figure 8. As mentioned in,[27](#)the deflection requirement for a railway bridge for serviceability limit state under live load plus dynamic load allowance requires that the deflection must not be greater than 1/640 of the span. It is obvious that deflection in this analysis is not a safety issue.

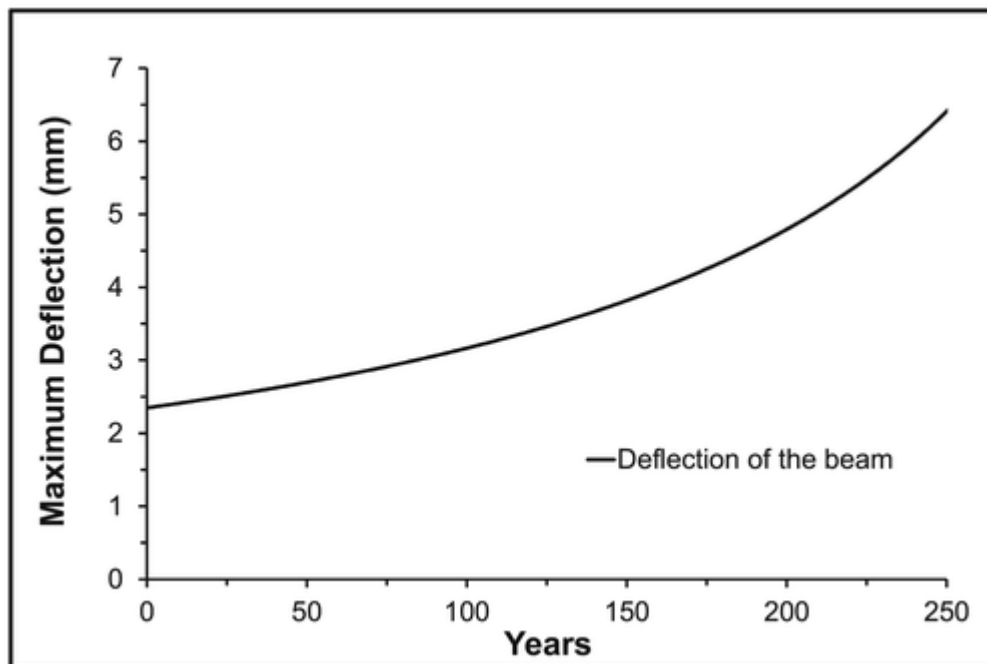


Figure 8

[Open in figure viewerPowerPoint](#)

Increase in maximum deflection with time

The next stage of this study used the finite element model to analyse the 4.87-m section of the track between the supports and to use the resultant stresses to compute crack growth. For simplicity, the loading applied to the model was based on a worst case scenario which was associated with an ore train (ie, a G Class locomotive with 20 fully loaded wagons) transiting the bridge. The G Class locomotive has the following specifications: Total weight = 128 tonnes, axle loading = 21.3 tonnes, wheel base = 3810 mm, axle spacing = 1905 mm, and leading wheel leading bogie to leading wheel trailing bogie = 12 622 mm. Due to symmetry considerations, only a quarter of the I beam was modelled. The resultant mesh, which was created using the software program FEMAP,[28](#)had 18 146 twenty-one-noded elements and 91 590 nodes (with a total of 274 770 degrees of freedom), see Figure 9. The stresses at the critical region were in reasonably good agreement with the results obtained from the field strain gauges measurements presented in Section 3 and discussed in more detail in.[29](#)

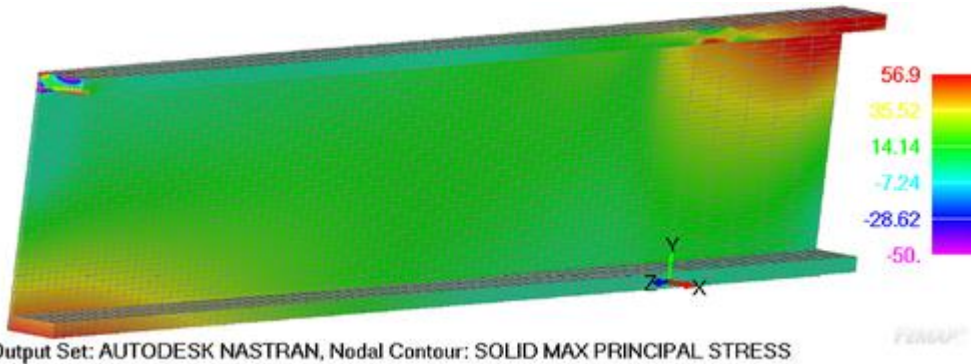


Figure 9

[Open in figure viewerPowerPoint](#)

The maximum principal stress plotting [Colour figure can be viewed at wileyonlinelibrary.com]

The resultant crack growth histories for the case of no corrosion and (allowing for) corrosion are given in Figure 10. In the coupled “corrosion-fatigue” analysis, if the crack growth in a year is less than 0.024 mm, it is assumed that the crack has been “eaten” by corrosion and its length reset to its initial size of 0.05 mm. In this coupled analysis, the section thickness continually reduces with time, ie, as the loss of metal increases, and the stresses increase accordingly. This coupled analysis yielded a life to failure of approximately 81 years. As such, there is a difference of ~18% in the computed fatigue life between the no corrosion and the coupled “corrosion-fatigue” analyses.

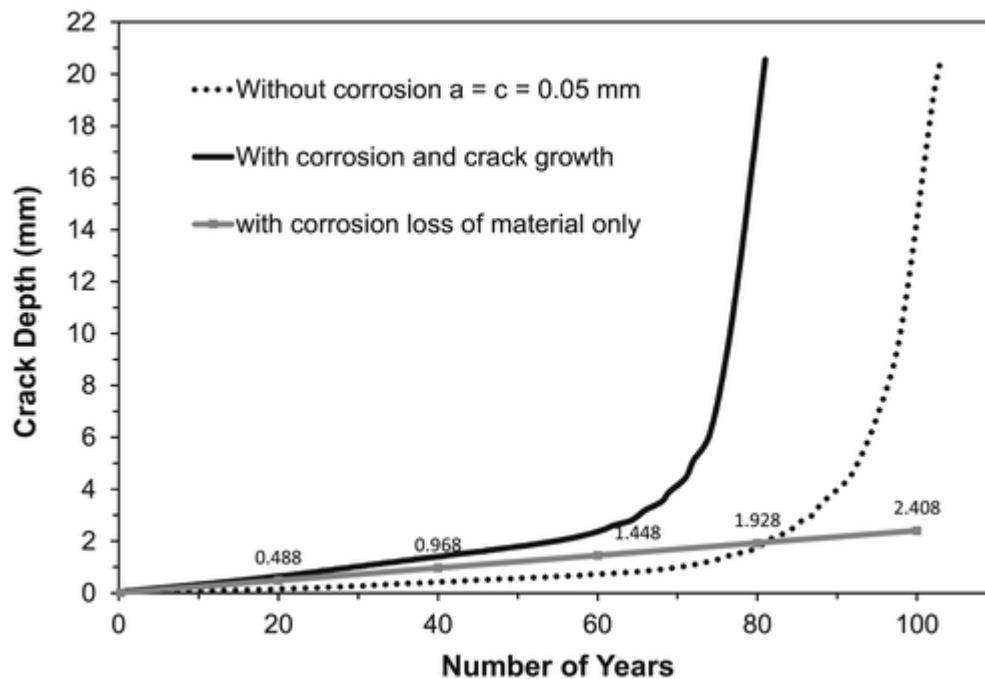


Figure 10

[Open in figure viewerPowerPoint](#)

The resultant computed crack growth histories ($a_i = c_i = 0.05$ mm)

It is reported in⁴ that the initial crack lengths found in the fatigue test on a specimen cut from a badly corroded bridge varied from approximately 0.1 to 1 mm.⁴ For a 1-mm initial crack, the difference between the 2 analyses is still significant (approximately 11%), see Figure 11.

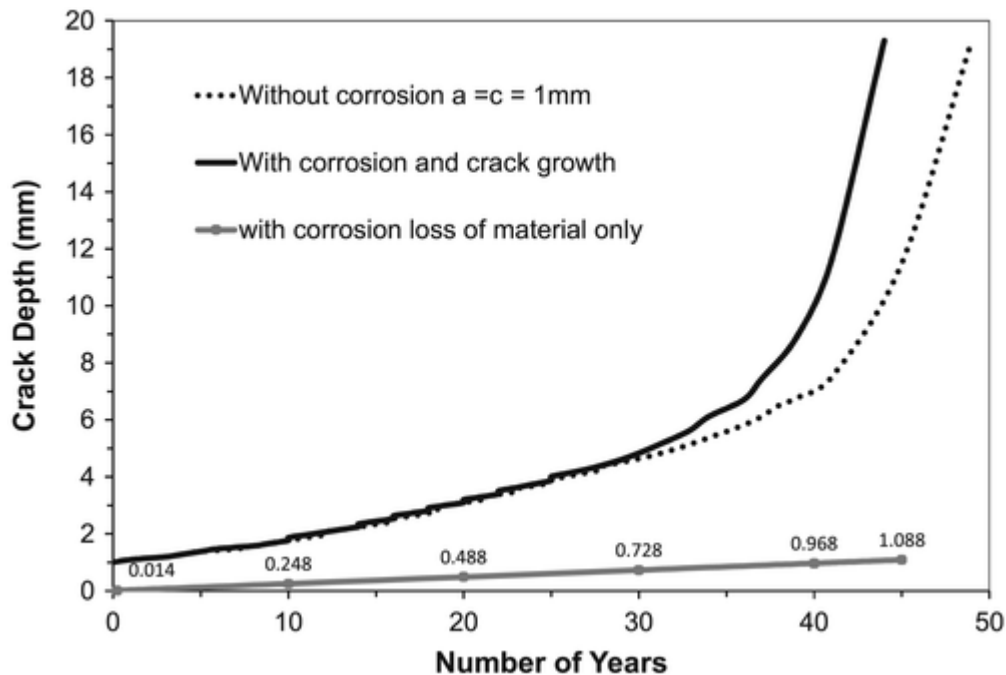


Figure 11

[Open in figure viewerPowerPoint](#)

The resultant computed crack growth histories ($a_i = c_i = 1$ mm)

Because the life of the bridge is a strong function of the size of the initiating (inherent) defect, the analysis was repeated for a range of initial crack sizes and the resulting lives are shown in Figure 12. This analysis revealed that the percentage difference between the case of no corrosion and the coupled “corrosion-fatigue” analysis reduces as the size of initial (inherent) crack is increased. It would also appear that, as a first approximation, the remaining life can be expressed as a logarithmic function of the initial flaw size.

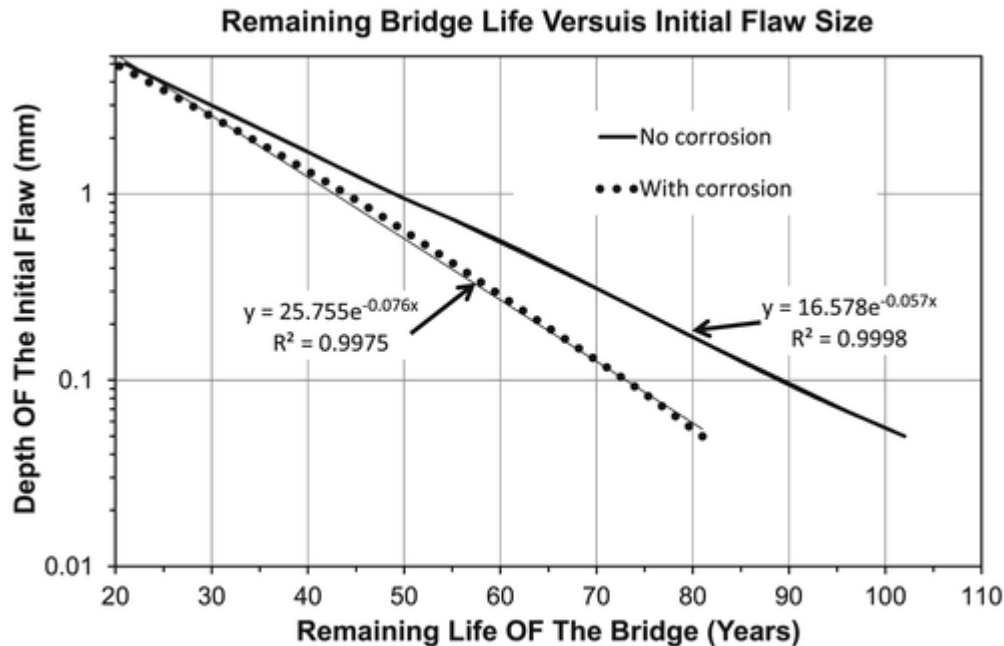


Figure 12

[Open in figure viewerPowerPoint](#)

Effect of the depth of the crevice on the remaining life of the bridge

6 CONCLUSIONS

This paper has presented a methodology that can be used to compute the growth of cracks that arise due to natural corrosion in bridge steels. A simplified analysis of V/Line Bridge 62 has been used to illustrate the need to perform a coupled corrosion-fatigue analysis.

Furthermore, comparing the life obtained by allowing only for corrosion and by performing a coupled corrosion-fatigue analysis, we find that:

- a. Life allowing for corrosion only = 244 years
- b. Life allowing for the coupled effect of corrosion and fatigue = 81 years

Therefore, failure as a result of metal loss from only corrosion would appear to be unconservative. As such, the interaction between fatigue crack growth and the stress increase created by corrosion-induced section reduction should be considered when assessing the remaining life of steel bridges.

APPENDIX : THE HARTMAN-SCHIJE VARIANT OF THE NASGRO CRACK GROWTH EQUATION

The NASGRO crack growth equation³⁰ is now perhaps the most widely used crack growth equation and as such is used in most commercially available computer codes, viz: FASTRAN, NASGRO, and AFGROW. The NASGRO equation³⁰ can be written in the form:

$$\begin{aligned} da/dN &= D [(1-f)/(1-R)]^m \Delta K^{(m-p)} (\Delta K - \Delta K_{thr})^p / (1-K_{max}/A)^q \\ &= D \Delta K_{eff}^{(m-p)} (\Delta K_{eff} - \Delta K_{eff,thr})^p / (1-K_{max}/A)^q (1) \end{aligned} \quad (A1)$$

where D is a constant, $f = K_{op}/K_{max}$, and the terms ΔK_{thr} and A are best interpreted as parameters chosen so as to fit the measured da/dN versus ΔK data. As explained in,⁸ the NASGRO equation contains the Hartman-Schijve crack growth equation, viz:

$$da/dN = D (\Delta K_{eff} - \Delta K_{eff,thr})^p / (1-K_{max}/A)^{p/2} \quad (A2)$$

as a special case, ie, $m = p$ and $q = p/2$. (Here $\Delta K_{eff,thr}$ is the associated effective threshold value of ΔK_{thr} .)